Available online at www.sciencedirect.com

ScienceDirect

Advances in Climate Change Research 8 (2017) 185–198

www.keaipublishing.com/en/journals/accr/

Downscaled climate change projections for the Hindu Kush Himalayan region using CORDEX South Asia regional climate models

Jayanarayanan SANJAY[a,*], Raghavan KRISHNAN[a], Arun Bhakta SHRESTHA[b], Rupak RAJBHANDARI[c], REN Guo-Yu[d]

[a] *Centre for Climate Change Research, Indian Institute of Tropical Meteorology, Pune 411008, India*
[b] *International Centre for Integrated Mountain Development, Kathmandu 3226, Nepal*
[c] *Department of Meteorology, Tri-Chandra Campus, Tribhuvan University, Kathmandu 3226, Nepal*
[d] *Laboratory for Climate Studies, National Climate Center, China Meteorological Administration, Beijing 100081, China*

Received 15 April 2017; revised 10 August 2017; accepted 14 August 2017
Available online 19 August 2017

Abstract

This study assessed the regional climate models (RCMs) employed in the Coordinated Regional climate Downscaling Experiment (CORDEX) South Asia framework to investigate the qualitative aspects of future change in seasonal mean near surface air temperature and precipitation over the Hindu Kush Himalayan (HKH) region. These RCMs downscaled a subset of atmosphere ocean coupled global climate models (AOGCMs) in the Coupled Model Intercomparison Project phase 5 (CMIP5) to higher 50 km spatial resolution over a large domain covering South Asia for two representation concentration pathways (RCP4.5 and RCP8.5) future scenarios. The analysis specifically examined and evaluated multi-model and multi-scenario climate change projections over the hilly sub-regions within HKH for the near-future (2036–2065) and far-future (2066–2095) periods. The downscaled multi-RCMs provide relatively better confidence than their driving AOGCMs in projecting the magnitude of seasonal warming for the hilly sub-region within the Karakoram and northwestern Himalaya, with higher projected change of 5.4 °C during winter than of 4.9 °C during summer monsoon season by the end of 21st century under the high-end emissions (RCP8.5) scenario. There is less agreement among these RCMs on the magnitude of the projected warming over the other sub-regions within HKH for both seasons, particularly associated with higher RCM uncertainty for the hilly sub-region within the central Himalaya. The downscaled multi-RCMs show good consensus and low RCM uncertainty in projecting that the summer monsoon precipitation will intensify by about 22% in the hilly sub-region within the southeastern Himalaya and Tibetan Plateau for the far-future period under the RCP8.5 scenario. There is low confidence in the projected changes in the summer monsoon and winter season precipitation over the central Himalaya and in the Karakoram and northwestern Himalaya due to poor consensus and moderate to high RCM uncertainty among the downscaled multi-RCMs. Finally, the RCM related uncertainty is found to be large for the projected changes in seasonal temperature and precipitation over the hilly sub-regions within HKH by the end of this century, suggesting that improving the regional processes and feedbacks in RCMs are essential for narrowing the uncertainty, and for providing more reliable regional climate change projections suitable for impact assessments in HKH region.

Keywords: CMIP5; CORDEX South Asia; Regional climate models; Hindu Kush Himalayan; Climate change projections

1. Introduction

The high mountains covering the Hindu Kush Himalayan (HKH) region has two distinct climatic regimes with the central and eastern Himalayan mountains receiving major part (up to 80%) of annual precipitation during the Indian summer monsoon months (June–September), while the winter westerly

* Corresponding author.
E-mail address: sanjay@tropmet.res.in (SANJAY J.).
Peer review under responsibility of National Climate Center (China Meteorological Administration).

http://dx.doi.org/10.1016/j.accre.2017.08.003

disturbances (from December to March) contributing to more than 50% of the precipitation over the western Himalaya and Hindu Kush mountains (Bookhagen and Burbank, 2010). This variability of weather patterns together with the confluence of different mountain ranges makes the topography of this area so complex that the relationship between rainfall and topography is poorly defined (Palazzi et al., 2013). These complex climatic regimes and geographical features pose a great challenge to climate models aiming to reproduce the observed climate and its variability. The numerous complexities in discerning precipitation trends within the HKH in recent decades using satellite rainfall estimates, reanalyses, and gridded in situ rain gauge data was illustrated by Palazzi et al. (2013). Their results indicated a statistically significant decreasing trend in Himalaya during summer. The water resources in HKH region are considered vulnerable to climate change due to the important role of snow and ice in the hydrology of the region (Barnett et al., 2005).

Panday et al. (2015) showed that the coarse-scale, multi-model ensembles of the coupled model intercomparison project phase 3 (CMIP3) and phase 5 (CMIP5) models are able to simulate the 20th century mean annual cycles of temperature and precipitation in the eastern and western Himalayan sub-regions within the HKH regions. However this study noted that these coupled atmosphere—ocean general circulation models (AOGCMs) indicate large spread in capturing the weather station based observational precipitation regimes over the HKH sub-regions. This evaluation study further discussed that the coarse-scale CMIP models were not able to resolve fine-scale processes and represent the complex topography in the western Himalayas. Hence these climate models could not realistically simulate the reductions in mean annual temperature (and therefore the decreasing trends in warm nights) observed across stations in the western Himalayas. Panday et al. (2015) suggested that higher resolution dynamical downscaling techniques using regional climate models (RCMs) that improve upon the topographic representation of this region are necessary to resolve the complexities of the monsoon and other hydrological processes over regional scales.

The application of RCMs to regions of complex topography remains challenging, partly due to their relatively coarse resolution in comparison to actual topography. However a RCM simulation forced with ERA-Interim atmospheric reanalyses (Dee et al., 2011) is found to represent well the role of steep topography on moisture transport fluxes and for the western Himalayas (Dimri et al., 2013). The RCMs forced with CMIP3 global climate models also capture the synoptic patterns influencing winter precipitation in the region (Wiltshire, 2014). However there are relatively few studies that aim to make a comprehensive assessment of climate projections for the Himalayan region. The RCM scenarios provided by the Providing Regional Climates for Impacts Studies (PRECIS) model for the eastern Himalaya projected a 4.3 °C increase in annual mean temperature and 34% increase in annual precipitation for SRES A2 scenario by the 2080s (Shrestha and Devkota, 2010). The Hadley Centre Regional Model 3 (HadRM3) used to downscale two CMIP3 global climate model simulations for the SRES A1B scenario projected that the HKH region will warm by 4–5.5 °C by 2080s (Wiltshire, 2014).

The World Climate Research Programme (WCRP) initiative Coordinated Regional Downscaling Experiment (CORDEX; http://www.cordex.org/) has generated an ensemble of regional climate change projections for South Asia with high spatial resolution (50 km) by downscaling several CMIP5 AOGCM outputs using multiple RCMs. Sanjay et al. (2017) evaluated the ability of the CORDEX RCMs in simulating the general characteristics of the climate over South Asia by analysing the spatial variability, pattern correlation and root mean square error using a Taylor diagram. The results indicated that the geographical distribution of surface air temperature and seasonal precipitation in the present climate is strongly affected by the choice of the RCM and boundary conditions (i.e. driving AOGCMs), and the downscaled seasonal averages are not always improved. The use of these high resolution multi-RCM ensembles not only provides information about variability among model projections but also facilitates an opportunity to understand the sub regional behaviour of climate variability within HKH across models and scenarios. The climate change impact analysis studies will require this climate information with regional details; however it is also important to evaluate the state-of-the-art AOGCMs used in CMIP5 to downscale using RCMs since the limitations and uncertainty inherent in these global climate simulations are inevitably transferred to the regional results (Sanjay et al., 2017). Hence this study uses CORDEX South Asia RCMs and their driving CMIP5 AOGCMs to examine their ability to represent the 20th century climate and analyse the evolution of seasonal mean temperature and precipitation into the future over the HKH region under different forcing conditions.

Section 2 describes the data and methods used. Results are discussed in Sections 3, while summary and conclusions are presented in Section 4.

2. Data and methods

The climate modelling groups around the world have contributed to a coordinated set of the 20th and 21st century climate simulations for CMIP5 (Taylor et al., 2012). These coarse-scale global climate projections have been dynamically downscaled to a uniform 50 km spatial resolution using RCMs over the large domain (19.25°–116.25°E; 15.75°S–45.75°N) covering CORDEX South Asia (Sanjay et al., 2017). The Centre for Climate Change Research (CCCR; http://cccr.tropmet.res.in) at the Indian Institute of Tropical Meteorology (IITM), the nodal agency for CORDEX South Asia, has archived selected climate parameters from these RCM outputs, which were shared by the modelling centres participating in CORDEX South Asia. These high resolution datasets for South Asia region are disseminated to users by publishing on the CCCR-IITM Climate Data Portal (http://cccr.tropmet.res.in/home/cordexsa_datasets.jsp) to assist the science community in conducting studies of climate change impacts at regional scales,

and to enhance public understanding of possible future climate patterns at the spatial scale of homogenous regions.

The CORDEX South Asia partners have recently published quality assured RCM outputs on the ESGF data nodes following CORDEX archive specifications (http://is-enes-data.github.io/cordex_archive_specifications.pdf). This study uses thirteen downscaled RCM outputs available on ESGF, of which six members each are contributed by CCCR-IITM and SMHI Sweden respectively, and included one member contribution from CSC Germany. The details of these CORDEX South Asia climate change experiments using three RCMs and their ten driving CMIP5 AOGCMs are listed in Table 1. These RCMs describe the atmosphere and its coupling with the land surface with differing dynamics and physics formulations (Giorgi et al., 2012; Samuelsson et al., 2011; Teichmann et al., 2013). For each experiment the historical runs, forced by observed natural and anthropogenic atmospheric composition, cover the period from 1950 until 2005. The future projections (2006–2100) are forced with two Representative Concentration Pathways (RCP), namely; RCP4.5 (mid-range emissions) and RCP8.5 (high-end emissions) scenarios, which prescribe future atmospheric greenhouse gas concentrations and aerosols. In this study we analyse the projected seasonal ensemble mean climate change as simulated by the CORDEX South Asia RCMs and their driving CMIP5 AOGCMs (except ICHEC-EC-EARTH) over the region (60°–105°E, 20°–40°N) covering HKH in near-future (2036–2065) and far-future (2066–2095) periods with reference to a baseline period (1976–2005) for the summer monsoon (June–September, JJAS) and winter (December–February, DJF) seasons. The confidence in the projected seasonal precipitation change is assessed based on the consensus on the sign of the change among the individual models. When more than 75% of the realizations concur then the sign of projected precipitation change is considered to be reliable. Additionally, in order to bring out the climatic responses in different parts of the hilly sub-regions within HKH, the area averaged summary statistics for the spread in the individual model simulated seasonal mean biases for the baseline

Table 1
List of the 13 CORDEX South Asia RCM simulations forced with 10 CMIP5 AOGCMs.

CORDEX South Asia RCM	RCM description	Contributing CORDEX Modelling Centre	Driving CMIP5 AOGCM (see details at https://verc.enes.org/data/enes-model-data/cmip5/resolution)	Contributing CMIP5 Modelling Centre
IITM-RegCM4 (6 members)	The Abdus Salam International Centre for Theoretical Physics (ICTP) Regional Climatic Model version 4 (RegCM4; Giorgi et al., 2012)	Centre for Climate Change Research (CCCR), Indian Institute of Tropical Meteorology (IITM), India	CCCma-CanESM2	Canadian Centre for Climate Modelling and Analysis (CCCma), Canada
			NOAA-GFDL-GFDL-ESM2M	National Oceanic and Atmospheric Administration (NOAA), Geophysical Fluid Dynamics Laboratory (GFDL), USA
			CNRM-CM5	Centre National de Recherches Me'téorologiques (CNRM), France
			MPI-ESM-MR	Max Planck Institute for Meteorology (MPI-M), Germany
			IPSL-CM5A-LR	Institut Pierre-Simon Laplace (IPSL), France
			CSIRO-Mk3.6	Commonwealth Scientific and Industrial Research Organization (CSIRO), Australia
SMHI-RCA4 (6 members)	Rossby Centre regional atmospheric model version 4 (RCA4; Samuelsson et al., 2011)	Rossby Centre, Swedish Meteorological and Hydrological Institute (SMHI), Sweden	ICHEC-EC-EARTH	Irish Centre for High-End Computing (ICHEC), European Consortium (EC)
			MIROC-MIROC5	Model for Interdisciplinary Research On Climate (MIROC), Japan Agency for Marine-Earth Sci. & Tech., Japan
			NOAA-GFDL-GFDL-ESM2M	NOAA, GFDL, USA
			CNRM-CM5	CNRM, France
			MPI-ESM-LR	MPI-M, Germany
			IPSL-CM5A-MR	IPSL, France
MPI-CSC-REMO2009 (1 member)	MPI Regional model 2009 (REMO 2009; Teichmann et al., 2013)	Climate Service Center (CSC), Germany	MPI-ESM-LR	MPI-M, Germany

reference period and the projected future changes in the northwest Himalaya and Karakoram (HKH1; 71°–79°E, 32°–39°N), the central Himalaya (HKH2; 76°–93°E, 27°–32°N) and the southeast Himalaya and Tibetan Plateau (HKH3; 93°–103°E, 28°–36°N) are separately analysed using grid cells within each sub-region above 2500 m a.s.l. (Fig. 1).

The high-resolution (0.5° × 0.5° latitude–longitude) daily gridded precipitation datasets based on rain-gauge observations available from APHRODITE's Water Resources (Asian Precipitation-Highly-Resolved Observational Daily Integration Towards Evaluation of Water Resources; Yatagai et al., 2012) for the period 1951–2007 over the monsoon Asia domain is used as the reference data for evaluation of the seasonal rainfall simulations over the HKH region during the baseline period 1976–2005. The high resolution (0.5° × 0.5° latitude–longitude) daily mean gridded temperature dataset based on station observations available for the period 1961–2007 over the monsoon Asia domain (Yasutomi et al., 2011) is used for evaluating the seasonal mean surface air temperature simulations over HKH region during the baseline period.

3. Results and discussion

3.1. Seasonal climatology over HKH

The spatial distribution of summer monsoon (JJAS) and winter (DJF) season near surface air temperature and rainfall climatology for the baseline period are analysed based on the APHRODITE gridded observations over a large region that includes HKH (Fig. 2). The seasonal mean temperature in the HKH region ranges between 0 °C and 10 °C during summer (Fig. 2a) and varies in winter (Fig. 2c) from around 10 °C in the plains south of HKH to less than −20 °C over Himalayan ranges with elevation above 5000 m. The summer season rainfall ranges spatially from less than 1 mm d^{-1} over the western part to more than 12 mm d^{-1} in the eastern parts of HKH region (Fig. 2b). The winter season rainfall over the Himalayas is considerably lower than the amounts received during summer monsoon except over the north-western stretch and Karakoram ranges, where it is relatively wet due to the influence of eastward propagating mid-latitude weather systems (Fig. 2d). Thus APHRODITE estimates over HKH are able to show the important seasonal features of the regional climate discussed in earlier studies (e.g., Palazzi et al., 2013; Kapnick et al., 2014). However Palazzi et al. (2013) noted that the APHRODITE provides only liquid phase rainfall estimates based on rain gauge station data, which could lead to an underestimation of the total precipitation, particularly in snow-rich areas such as the HKH and especially in winter.

The spatial distribution of the CORDEX South Asia multi-RCM bias in near surface air temperature and precipitation seasonal ensemble mean climatology for the baseline period relative to APHRODITE observations are shown in Fig. 3. The simulated 2-m air temperature climate shows large cold bias over HKH region in both seasons. The summer monsoon seasonal mean differences are generally smaller than 1 °C over most of the Indian region (Fig. 3a), although differences above 2 °C exist in parts of north India and the adjoining HKH region. The winter season show relatively higher cold biases than during the summer monsoon even over the Indian region (Fig. 3c). The evaluation of the CMIP5 multi-AOGCM annual mean surface air temperature in the fifth assessment report of the Intergovernmental Panel on Climate Change (IPCC) also

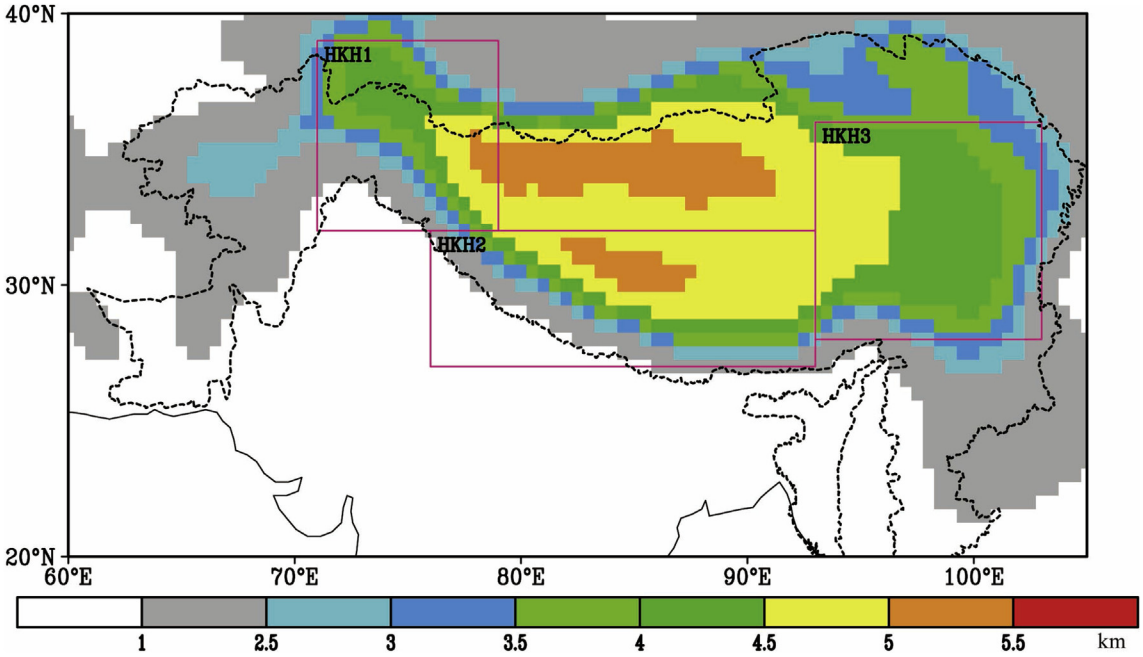

Fig. 1. IITM-RegCM4 RCM elevation (km) over the region covering HKH, with parts of the hilly sub-regions within HKH defined by grid cells in each box above 2500 m a.s.l. (non-greyscale): northwest Himalaya and Karakoram (HKH1); central Himalaya (HKH2); southeast Himalaya and Tibetan Plateau (HKH3). The HKH boundary is shown with dashed line.

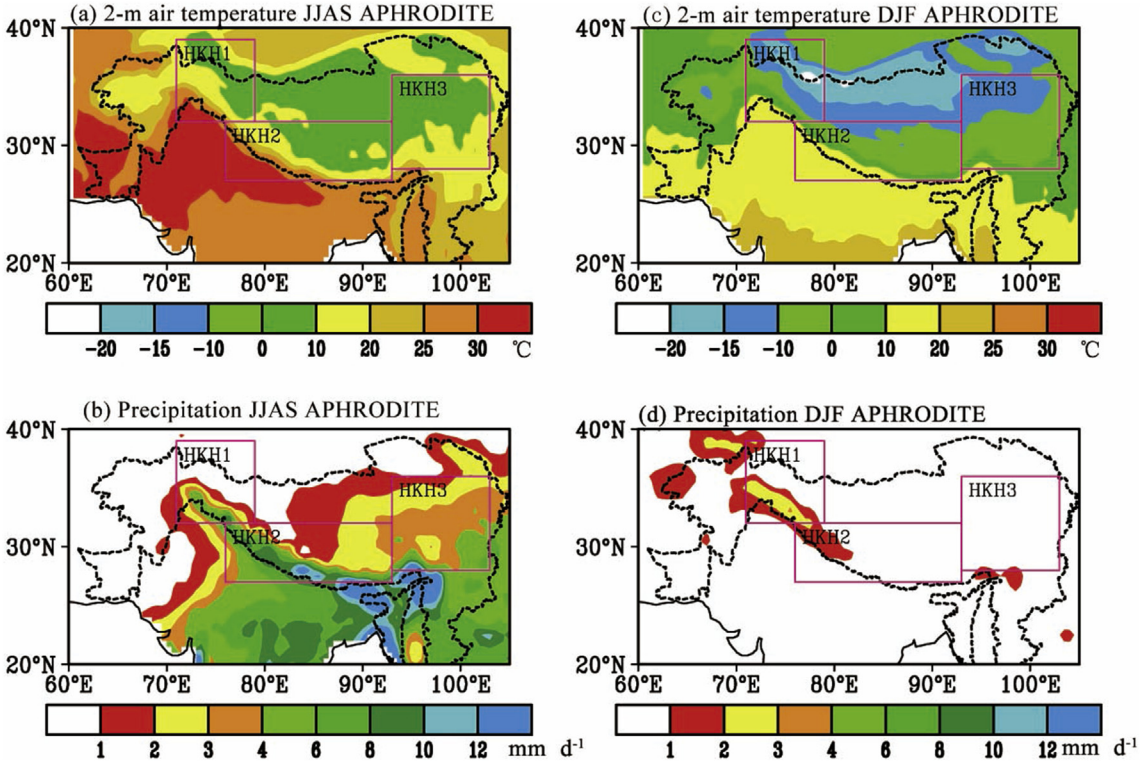

Fig. 2. Spatial distribution of the seasonal mean climatology during 1976–2005 based on APHRODITE gridded observations for (top panels) surface air temperature (°C) and (bottom panels) total precipitation (mm d^{-1}) during (a–b) summer monsoon and (c–d) winter seasons. The HKH boundary is shown with dashed line. The boxes represent the three HKH sub-regions used for detailed analysis (see text).

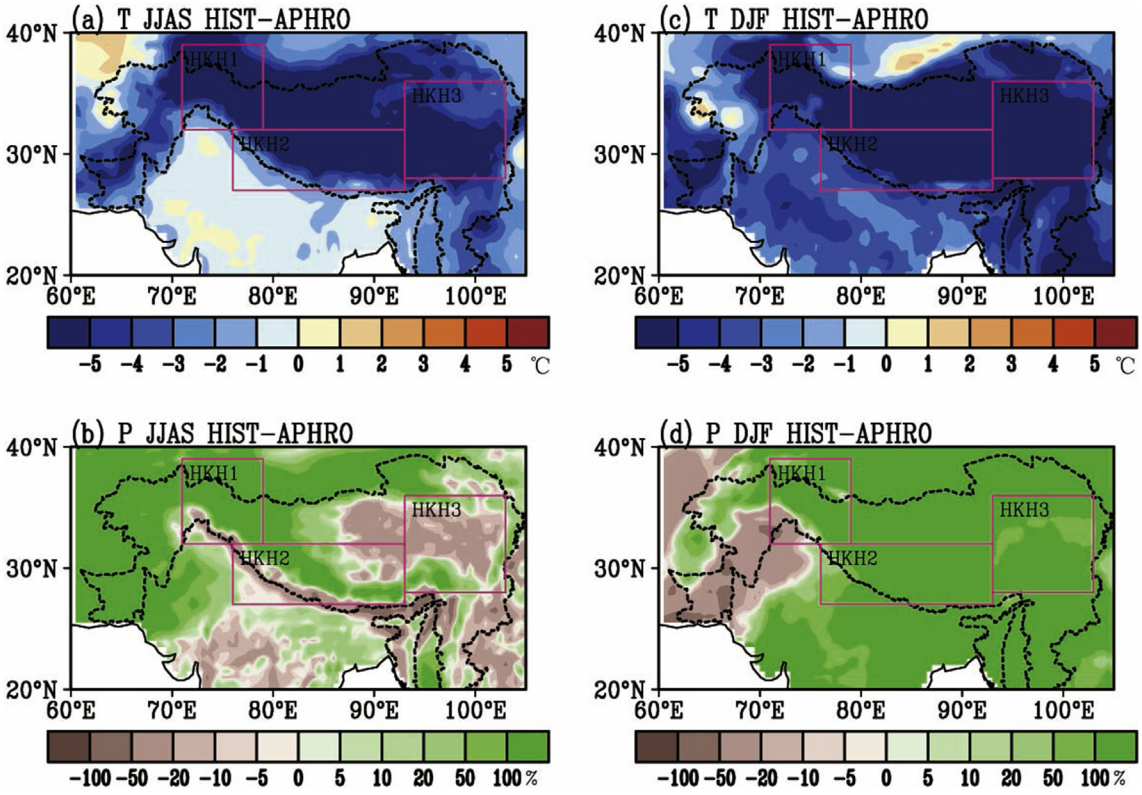

Fig. 3. Spatial distribution of the CORDEX South Asia multi-RCM bias in seasonal ensemble mean climatology (1976–2005) relative to APHRODITE observations for (top panels) surface air temperature (°C) and (bottom panels) total precipitation (%) during (a–b) summer monsoon and (c–d) winter seasons. The HKH boundary is shown with dashed line. The boxes represent the three HKH sub-regions used for detailed analysis (see text).

noted that the biases are larger than 2 °C at high elevations over the Himalayas (Flato et al., 2013). The strong cold bias found in the Himalayan region was also partly attributed to the observation data sparseness in this region by an evaluation study of REMO RCM in the CORDEX framework (Jacob et al., 2012).

The multi-RCM ensemble mean total precipitation is largely overestimated over the higher elevations in the northwest Himalaya and Karakoram with low observed summer time precipitation (Fig. 3b). While along the southern slopes of the Himalaya and over the higher elevated regions in southeast Himalaya and the Tibetan Plateau the CORDEX RCM ensemble mean indicate dry bias during the summer monsoon season. The winter season total precipitation shows a wet bias over the entire HKH region and the adjoining India (Fig. 3d). The simulated lower temperatures may have resulted in the overestimation of snow with respect to rainfall in these RCMs, particularly during winter. It is also possible that the contribution of liquid-only rainfall from the APHRODITE observations might have resulted in underestimation of total precipitation during winter in this dataset. On the other hand, the overestimation of the snow cover and the related higher surface albedo during winter is probably the reason for larger cold bias in the RCMs during this season.

Fig. 4 shows that the observed summer monsoon season near surface air temperature is relatively warmer over the hilly regions of northwest Himalaya and Karakoram (HKH1; 10.1 °C) than in the central Himalaya (HKH2; 9.5 °C) and southeast Himalaya and Tibetan Plateau (HKH3; 9.1 °C) during the baseline period. During winter season the observed temperature over HKH1 is relatively cooler (−12.3 °C) than over HKH2 (−7.0 °C) and HKH3 (−7.7 °C). These boxplots show that the systematic cold bias discussed earlier for the RCMs are also present for the AOGCMs in these three HKH sub-regions during both the seasons. However the AOGCMs show relatively less cold bias than the downscaled RCMs. The spread among the individual RCM simulated winter season temperature are also found to be higher than in the AOGCMs. Panday et al. (2015) had reported that the AOGCM simulated annual cycle of temperature indicated large cold bias in the hilly regions over western Himalaya of approximately 3.9 °C, particularly during the winter months. However their analysis using all grid points in the region found that most of the AOGCMs overestimated temperature by approximately 0.4 °C across all months in the eastern Himalayan region.

The observed seasonal mean precipitation (Fig. 4) during the summer monsoon is relatively less over the hilly regions in HKH1 (0.9 mm d^{-1}) than over HKH2 (2.8 mm d^{-1}) and HKH3 (3.3 mm d^{-1}). The winter precipitation is relatively higher over HKH1 (0.8 mm d^{-1}) than over HKH2 (0.3 mm d^{-1}) and HKH3 (0.2 mm d^{-1}) based on the APHRODITE observations. The earlier study by Panday et al. (2015) had also shown that the observed precipitation in the eastern Himalayan region has a strong seasonal cycle with most precipitation falling in the summer monsoon months, while the western Himalaya receives on average lower precipitation with only a small seasonal variability. The RCMs and the AOGCMs overestimate the total precipitation in these three HKH sub-regions during both the seasons. The RCM ensemble median is closer to observations over HKH2 and HKH3 for both seasons, and is also associated with smaller inter-model variability over central Himalaya during the summer monsoon season (Fig. 4e).

3.2. Future projections for HKH

The spatial pattern of the projected changes in seasonal ensemble mean near-surface air temperature based on the AOGCMs are shown for the near-future and far-future periods relative to the baseline period in the top panels of Figs. 5 and 7 respectively. The corresponding downscaled projected changes based on the RCMs are shown in the top panels of Figs. 6 and 8 respectively. The magnitude of the projected seasonal warming is found to vary with region, season, averaging period and scenario used for the AOGCMs and the RCMs. The seasonal temperature changes over the western region of HKH appears to be relatively higher (lower) than in the eastern region during the summer monsoon (winter) season for near-future and far-future periods under both scenarios. Table 2 shows the projected changes in the multi-RCM and multi-AOGCM seasonal ensemble mean near-surface air temperature averaged over the hilly regions of the three HKH sub-regions under RCP4.5 and RCP8.5 scenarios for near-future and far-future periods. This detailed analysis confirms that during summer monsoon (winter) season relatively higher (lower) warming will occur over the hilly regions of northwest Himalaya and Karakoram than in the central Himalaya and southeast Himalaya and Tibetan Plateau for both scenarios. The ensemble mean of the RCMs indicate relatively lower warming in summer monsoon season than the AOGCMs over these HKH sub-regions for both periods and scenarios. While the multi-RCM ensemble mean projected summer temperature changes for far-future period under RCP8.5 scenario varies from 4.9 °C over HKH1 to 4.2 °C over HKH3, the corresponding multi-AOGCM ensemble mean changes are relatively higher varying from 5.7 °C over HKH1 to 4.4 °C over HKH3. The ensemble mean winter season warming is relatively higher for RCMs than that projected by the AOGCMs over the three HKH sub-regions for the far-future period under RCP8.5 scenario. While the multi-RCM ensemble mean projected winter season changes for this scenario in the far-future period varies from 5.4 °C over HKH1 to 6.0 °C over HKH2, the corresponding multi-AOGCM ensemble mean changes are relatively lower varying from 5.1 °C over HKH1 to 5.8 °C over HKH2. Thus the analysis of high resolution downscaled RCMs suggest that the highest seasonal mean warming within the HKH region of 6.0 °C is expected over the central Himalaya during winter season by the end of 21st century under the high-end RCP8.5 scenario.

The spatial pattern of the seasonal ensemble mean projected percent changes in total precipitation based on the AOGCMs are shown for the near-future and far-future periods in the bottom panels of Figs. 5 and 7 respectively. The corresponding downscaled projected changes based on the RCMs

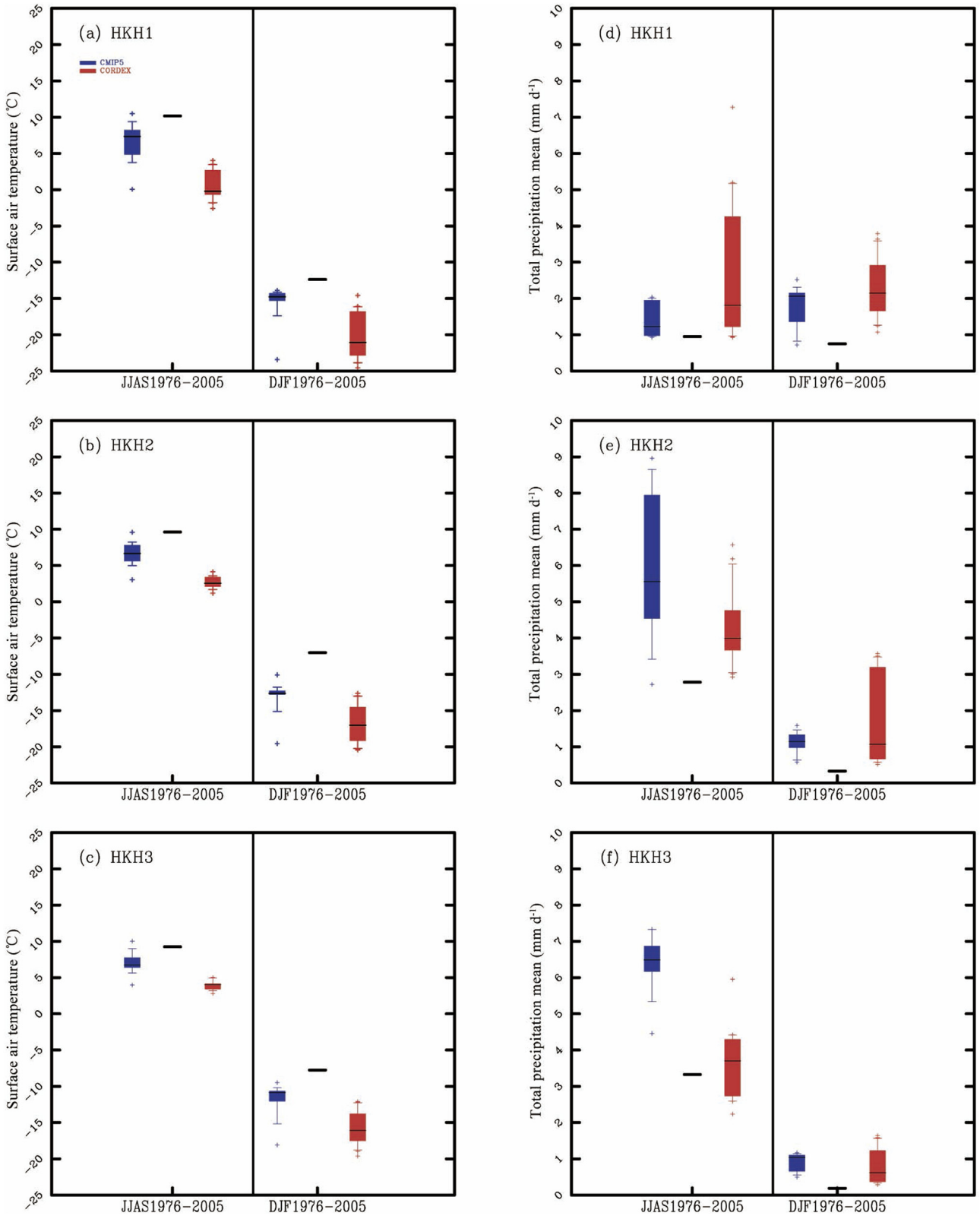

Fig. 4. Boxplots showing the (red colours) CORDEX RCMs and (blue colours) CMIP5 AOGCMs multi-model statistics for seasonal mean (left panels) surface air temperature (°C) and (right panels) total precipitation (mm d^{-1}) during (left sub-panels) summer monsoon and (right sub-panels) winter seasons in the three hilly sub-regions within HKH. The box represents the interquartile range (IQR) and the horizontal black line in each box is the multi-model median value. The whiskers represent the furthest model value within 1.5 times the IQR. The symbols show the outliers. The observed values based on APHRODITE are shown as a thick black line in the middle of each sub-panel.

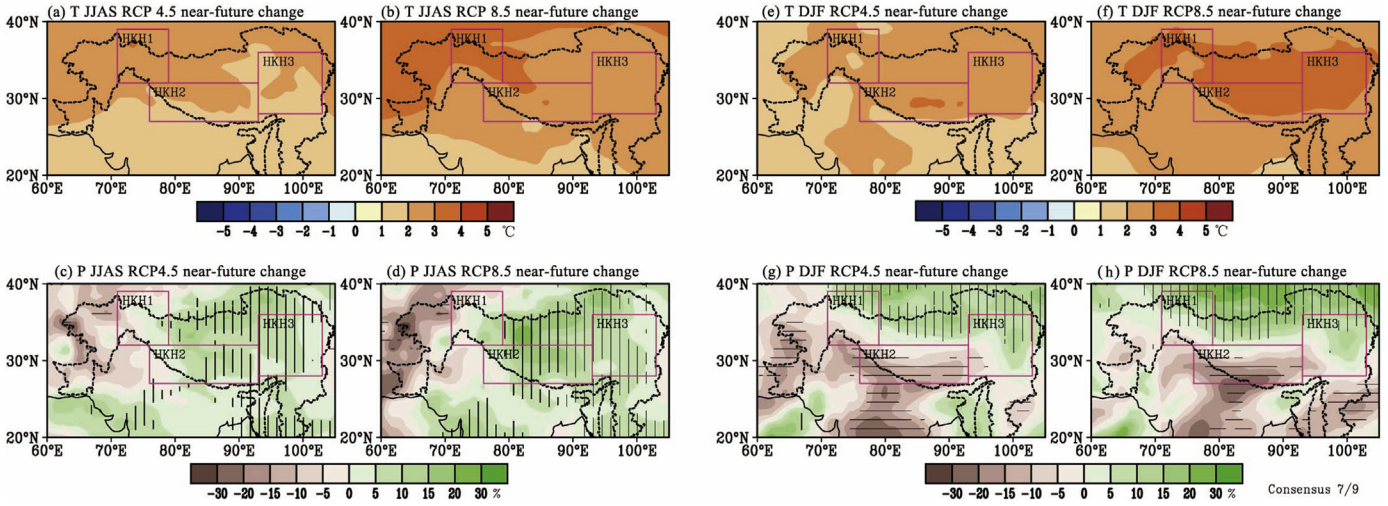

Fig. 5. Spatial distribution of climate change in CMIP5 multi-AOGCM seasonal ensemble mean in near-future ([2036–2065] – [1976–2005]) for (top panels) surface air temperature (°C) and (bottom panels) total precipitation (%) during (a–d) summer monsoon and (e–h) winter seasons for RCP4.5 and RCP8.5 scenarios. Ensemble mean of the CMIP5 AOGCMs used to downscale the CORDEX South Asia RCMs (listed in Table 1). Striping in bottom panels indicates where at least 7 out of the 9 realizations concur on an increase (vertical) or decrease (horizontal) in the future scenarios. The HKH boundary is shown with dashed line. The boxes represent the three hilly sub-regions within HKH used for detailed analysis (see text).

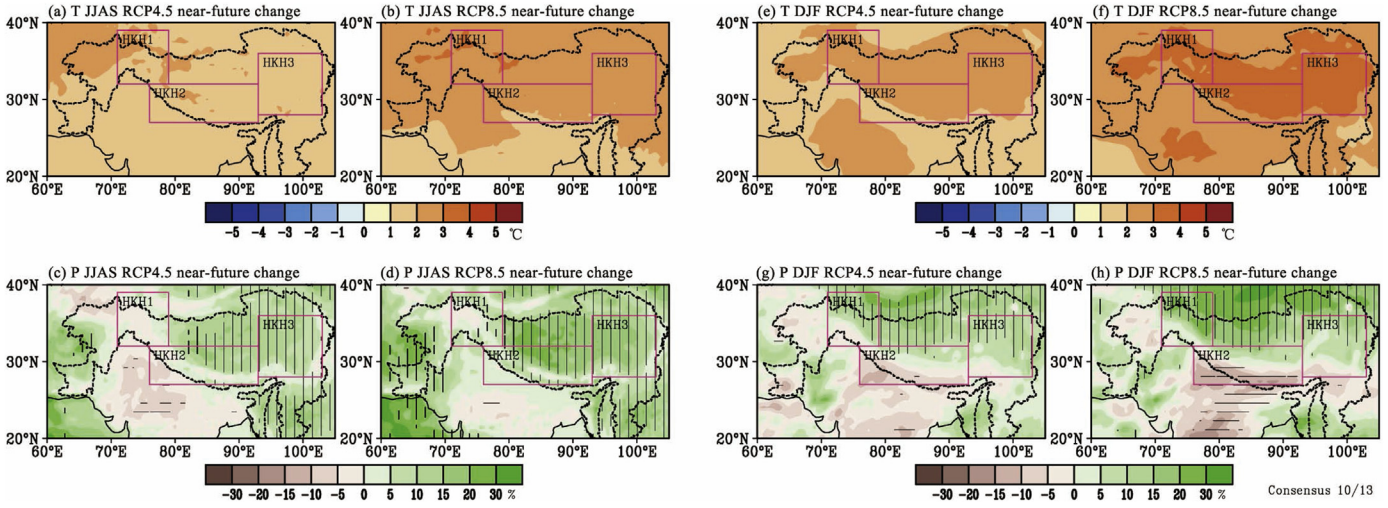

Fig. 6. Spatial distribution of climate change in CORDEX South Asia multi-RCM seasonal ensemble mean in near-future ([2036–2065] – [1976–2005]) for (top panels) surface air temperature (°C) and (bottom panels) total precipitation (%) during (a–d) summer monsoon and (e–h) winter seasons for RCP4.5 and RCP8.5 scenarios. Ensemble mean of the CORDEX South Asia RCMs dynamically downscaled from CMIP5 AOGCMs (listed in Table 1). Striping in bottom panels indicates where at least 10 out of the 13 realizations concur on an increase (vertical) or decrease (horizontal) in the future scenarios. The HKH boundary is shown with dashed line. The boxes represent the three hilly sub-regions within HKH used for detailed analysis (see text).

are shown in the bottom panels of Figs. 6 and 8 respectively. The magnitude and sign of the projected seasonal percent change is found to vary with region, season, averaging period and scenario used. The striping indicates where more than 75% of the realizations concur on an increase (vertical) or decrease (horizontal) in total precipitation for the RCPs. The individual RCMs agree on projected summer season increase in precipitation over the hilly regions in central Himalaya (HKH2) and southeast Himalaya and Tibetan Plateau (HKH3) for both RCP4.5 and RCP8.5 scenarios in the near-future and far-future periods. The models show low agreement in the southern slopes of the Himalaya and in the northwest Himalaya and Karakoram (HKH1) region during the summer season for both scenarios till the end of 21st century. The models agree well on the winter season increase in total precipitation over HKH1 for near-future and far-future periods and for both scenarios. However the consensus among the models for projected reduction in winter precipitation over HKH2 and HKH3 are low for both scenarios in the two periods. Table 3 shows the projected percent changes in the multi-RCM and multi-AOGCM seasonal ensemble mean total precipitation averaged over the hilly regions of the three HKH sub-regions (see Fig. 1) with RCP4.5 and RCP8.5 scenarios for near-future and far-future periods. This detailed analysis

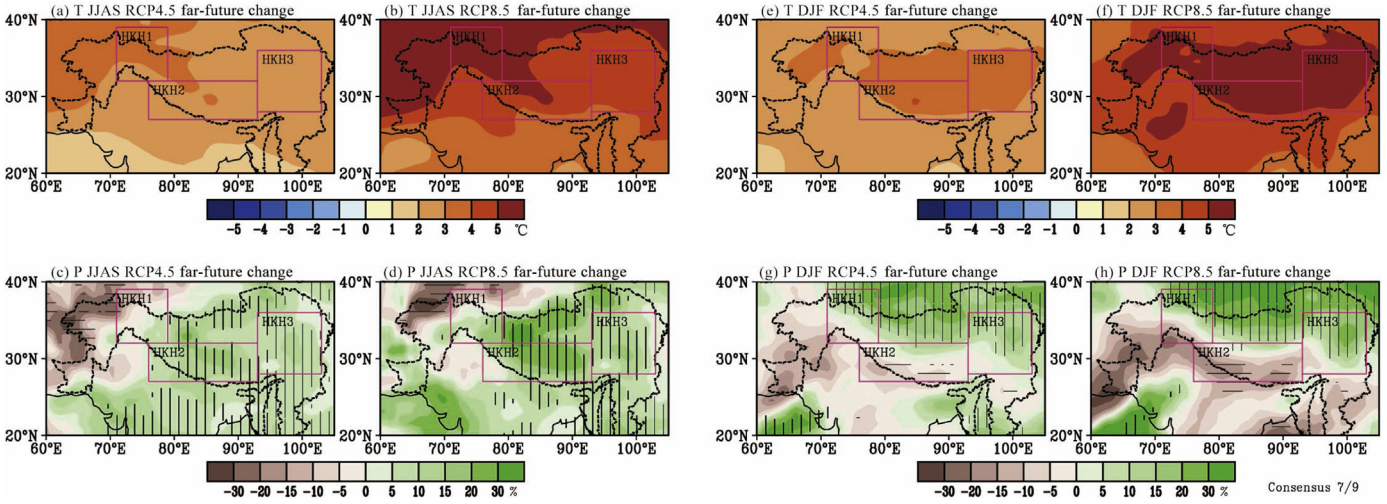

Fig. 7. Spatial distribution of climate change in CMIP5 multi-AOGCM seasonal ensemble mean in far-future ([2066–2095] – [1976–2005]) for (top panels) surface air temperature (°C) and (bottom panels) total precipitation (%) during (a–d) summer monsoon and (e–h) winter seasons for RCP4.5 and RCP8.5 scenarios. Ensemble mean of the CMIP5 AOGCMs used to downscale the CORDEX South Asia RCMs (listed in Table 1). Striping in bottom panels indicates where at least 7 out of the 9 realizations concur on an increase (vertical) or decrease (horizontal) in the future scenarios. The HKH boundary is shown with dashed line. The boxes represent the three hilly sub-regions within HKH used for detailed analysis (see text).

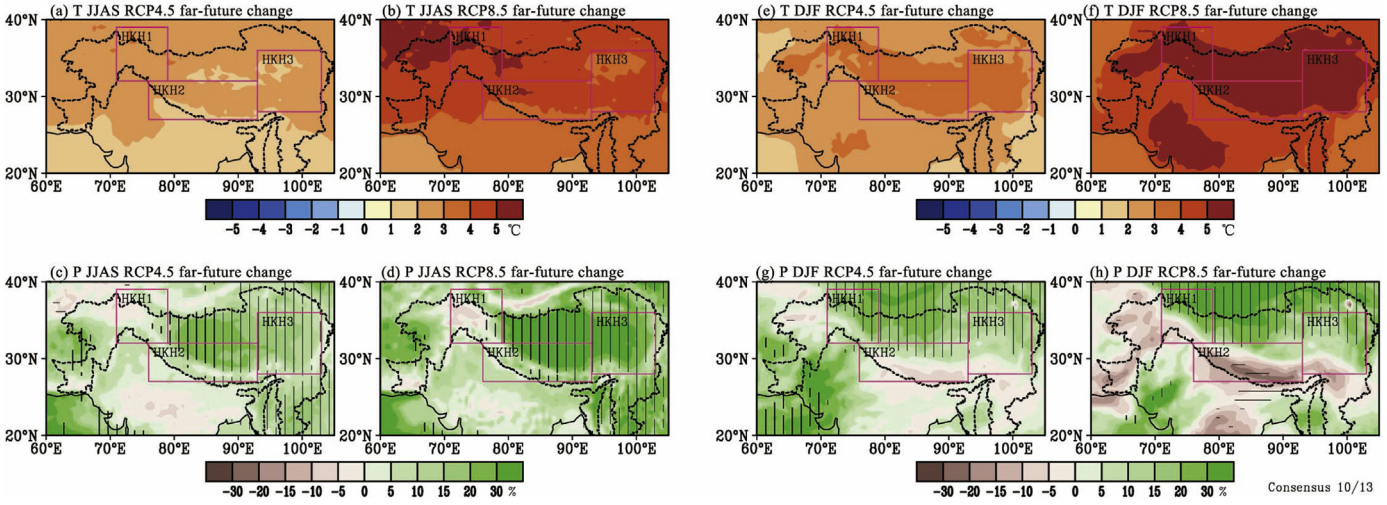

Fig. 8. Spatial distribution of climate change in CORDEX South Asia multi-RCM seasonal ensemble mean in far-future ([2066–2095] – [1976–2005]) for (top panels) surface air temperature (°C) and (bottom panels) total precipitation (%) during (a–d) summer monsoon and (e–h) winter seasons for RCP4.5 and RCP8.5 scenarios. Ensemble mean of the CORDEX South Asia RCMs dynamically downscaled from CMIP5 AOGCMs (listed in Table 1). Striping in bottom panels indicates where at least 10 out of the 13 realizations concur on an increase (vertical) or decrease (horizontal) in the future scenarios. The HKH boundary is shown with dashed line. The boxes represent the three hilly sub-regions within HKH used for detailed analysis (see text).

Table 2
Seasonal ensemble mean projected changes in near-surface air temperature (°C) relative to 1976–2005 in three hilly sub-regions within HKH (see Fig. 1): northwest Himalaya and Karakoram (HKH1); central Himalaya (HKH2); southeast Himalaya and Tibetan Plateau (HKH3).

Scenario	Period	Multi-model ensemble mean	Summer monsoon season (June–September)			Winter season (December–February)		
			HKH1	HKH2	HKH3	HKH1	HKH2	HKH3
RCP4.5	2036–2065	CORDEX RCMs	2.0	1.7	1.7	2.3	2.4	2.4
		CMIP5 AOGCMs	2.6	2.1	2.0	2.1	2.7	2.5
	2066–2095	CORDEX RCMs	2.6	2.2	2.2	3.1	3.3	3.1
		CMIP5 AOGCMs	3.3	2.7	2.5	3.0	3.6	3.3
RCP8.5	2036–2065	CORDEX RCMs	2.7	2.3	2.3	3.2	3.3	3.2
		CMIP5 AOGCMs	3.3	2.7	2.5	3.0	3.4	3.2
	2066–2095	CORDEX RCMs	4.9	4.3	4.2	5.4	6.0	5.6
		CMIP5 AOGCMs	5.7	4.7	4.4	5.1	5.8	5.4

Table 3
Seasonal ensemble mean projected changes in total precipitation (%) relative to 1976–2005 in three hilly sub-regions within HKH (see Fig. 1): northwest Himalaya and Karakoram (HKH1); central Himalaya (HKH2); southeast Himalaya and Tibetan Plateau (HKH3).

Scenario	Period	Multi-model ensemble mean	Summer monsoon season (June–September)			Winter season (December–February)		
			HKH1	HKH2	HKH3	HKH1	HKH2	HKH3
RCP4.5	2036–2065	CORDEX RCMs	−0.1	4.4	6.8	7.0	−0.7	3.1
		CMIP5 AOGCMs	0.8	6.7	4.6	1.0	−7.7	2.1
	2066–2095	CORDEX RCMs	3.5	10.5	10.4	14.1	1.5	3.7
		CMIP5 AOGCMs	−0.3	11.8	7.3	6.2	−0.7	5.5
RCP8.5	2036–2065	CORDEX RCMs	3.7	9.1	10.2	12.8	−1.3	0.9
		CMIP5 AOGCMs	3.6	10.7	5.7	5.1	−8.5	0.7
	2066–2095	CORDEX RCMs	3.9	19.1	22.6	12.9	−8.8	0.6
		CMIP5 AOGCMs	5.0	19.1	9.7	6.9	−8.1	6.0

further confirms that during summer (winter) relatively higher (lower) precipitation increase will occur over the hilly regions of central Himalaya and southeast Himalaya and Tibetan Plateau than in northwest Himalaya and Karakoram for both scenarios by the end of 21st century. The ensemble mean of the high resolution downscaled RCMs and the AOGCMs indicate similar variations in the projected summer monsoon season total precipitation changes across these HKH sub-regions for both periods and scenarios. The multi-RCM ensemble mean projected summer precipitation changes for far-future period under RCP8.5 scenario varies from 3.9% over HKH1 to 22.6% over HKH3, while the corresponding multi-AOGCM ensemble mean changes vary from 5.0% over HKH1 to 19.1% over HKH2. The ensemble mean winter season precipitation change over HKH1 is relatively higher for CORDEX RCMs (12.9%) than that projected by the CMIP5 AOGCMs (6.9%) for the far-future period under RCP8.5 scenario. While the multi-RCM ensemble mean projected winter season changes for this scenario in the far-future period varies from −8.8% over HKH2 to 12.9% over HKH1, the corresponding multi-AOGCM ensemble mean changes vary from −8.1% over HKH2 to 6.9% over HKH1. In summary, these high resolution downscaled projected changes in seasonal precipitation indicate intensification of the summer monsoon, particularly of about 22% in the southeast Himalaya and Tibetan Plateau region. The multi-RCM projections of seasonal precipitation also indicate a wetter cold season with about 14% and 13% increases in winter precipitation over the northwest Himalaya and Karakoram by the end of 21st century under the RCP4.5 and RCP8.5 scenarios respectively.

The boxplots in Fig. 9 summaries the degree of uncertainty in the projected changes of these seasonal ensemble mean near-surface air temperature and total precipitation arising from individual models and scenarios. The median warming is seen to be relatively lower during the summer monsoon season for the high resolution downscaled RCMs in comparison to the AOGCMs over the three HKH sub-regions for both periods and scenarios as was discussed earlier based on the seasonal ensemble mean temperature changes (Table 2). Further, the RCMs indicate smaller IQR than for the AOGCMs over the hilly regions of northwest Himalaya and Karakoram, suggesting less inter-model variability in the magnitude of the summer monsoon season temperature increase in this HKH sub-region. The RCMs also indicate better confidence with smaller IQR than AOGCMs in projecting relatively higher median winter warming for HKH1 compared to the summer monsoon season by the end of 21st century under RCP8.5 scenario. However the results summarized earlier based on the analysis of ensemble mean that the CORDEX RCMs suggest highest seasonal ensemble mean warming within the HKH region of 6.0 °C over the central Himalaya during winter season by the end of 21st century under the high-end RCP8.5 scenario, is associated with higher model uncertainty as shown by the relatively larger divergence among these RCMs than for the AOGCMs. The consensus found in the CORDEX multi-RCMs for projected summer monsoon season increase in ensemble mean precipitation over the hilly regions in southeast Himalaya and Tibetan Plateau (HKH3) for both RCP4.5 and RCP8.5 scenarios in the near-future and far-future periods (Table 3) is further confirmed by the seasonal median increase of similar magnitude. However the projected increase in median precipitation for this season over the hilly regions of central Himalaya (HKH2) is found to be associated with higher inter-model variability among the downscaled RCMs than for the AOGCMs. The less agreement among the RCMs on the projected increase in median precipitation during summer monsoon season in the hilly regions of northwest Himalaya and Karakoram (HKH1) by the end of 21st century under RCP8.5 scenario is also clearly depicted in the box plot statistics. The consensus showed by these models on the winter season increase in ensemble mean total precipitation over HKH1 for both future periods and for both scenarios is accompanied with moderate uncertainty as shown by the inter-model spread in the projected changes, particularly for the RCMs. Further the boxplots confirm the low agreement among the RCMs for projected reduction in winter ensemble mean precipitation over HKH2 and HKH3 as shown by the higher divergence among these models.

The seasonal ensemble mean projected changes in near-surface temperature over the three HKH sub-regions for the near-future and far-future periods discussed earlier (Table 2) are found to be relatively higher than the seasonal global means based on the same subset of CMIP5 AOGCMs

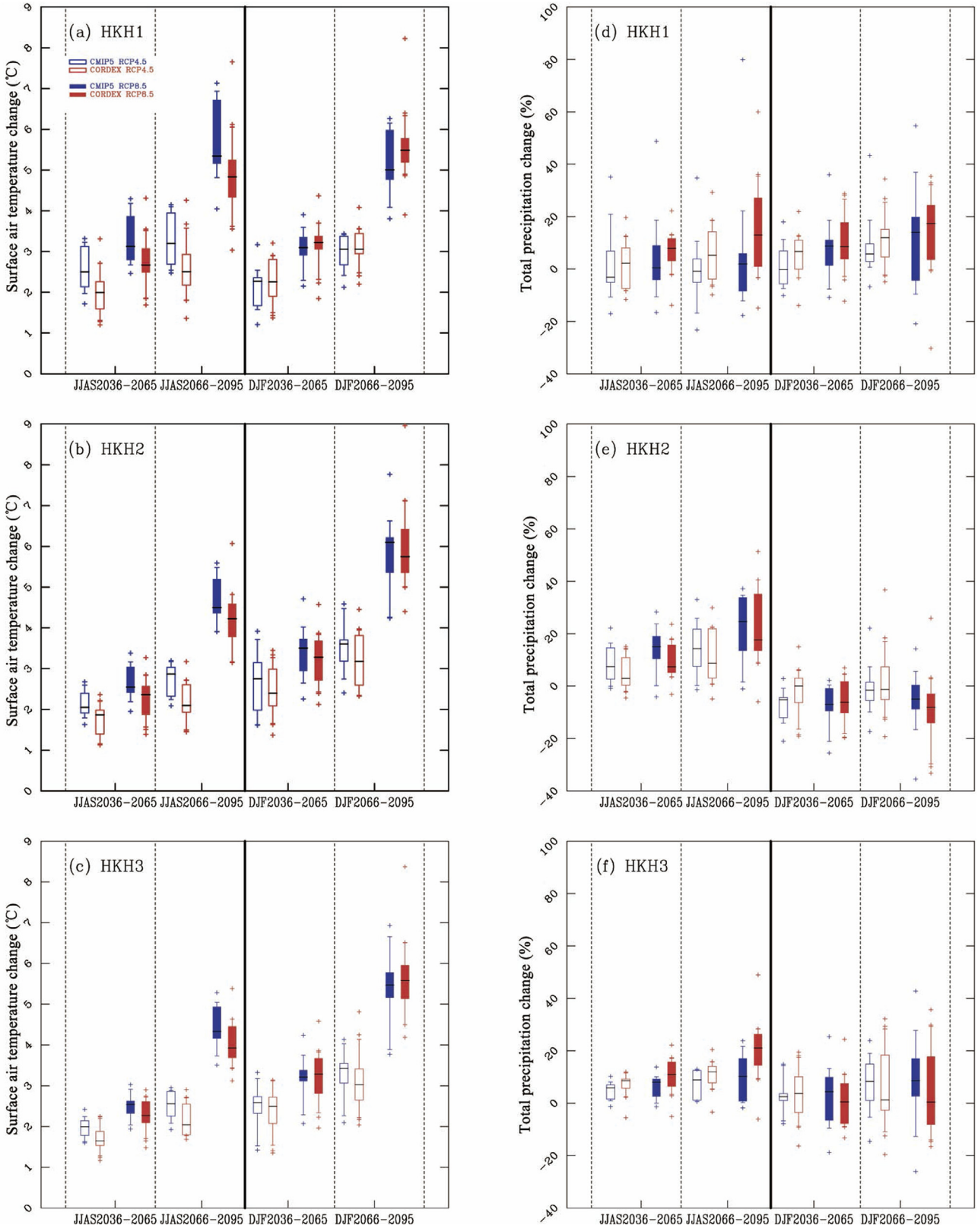

Fig. 9. Boxplots showing the (red colours) CORDEX RCMs and (blue colours) CMIP5 AOGCMs multi-model statistics for seasonal mean (left panels) surface air temperature (°C) and (right panels) total precipitation (%) changes during summer monsoon and winter seasons in the three hilly sub-regions within HKH (see Fig. 1). Each of the sub-panels show seasonal mean changes in near-future ([2036–2065] – [1976–2005]) and far-future ([2066–2095] – [1976–2005]) for (unfilled boxes) RCP4.5 and (filled boxes) RCP8.5 scenarios. The box represents the interquartile range (IQR) and the horizontal black lines represent the multi-model median values. The whiskers represent the furthest model value within 1.5 times the IQR. The symbols show the outliers.

(Table 4). The RCMs and the AOGCMs project summer monsoon season ensemble mean changes in the far-future period for RCP8.5 scenario over the HKH sub-regions ranging between 4.2 °C and 5.7 °C (Table 2). However the projected changes in the global mean surface air temperature during this season derived from the ensemble mean of the same sub-set of the AOGCMs is 3.3 °C only for this high emission scenario in the same far-future period (Table 4). These models indicate that the HKH sub-regions are projected to have higher temperature increases ranging between 5.1 °C and 6.0 °C during the winter season for the RCP8.5 scenario in this far-future period, while the corresponding projected changes in the global mean surface air temperature for this season derived from the CMIP5 multi-AOGCM sub-set is 3.5 °C only. Although the box plot analysis (Fig. 9) showed that the projected higher winter warming over the hilly regions of central Himalaya (HKH2) is associated with higher model uncertainty, the magnitude of warming is significantly higher than the projected global mean winter season temperature increases by the end of 21st century.

4. Summary and conclusions

The dynamically downscaled regional climate change projections using regional climate models (RCMs) available from the CORDEX South Asia are analysed to evaluate the future scenarios and possible trends in three sub-regions within the Hindu Kush Himalayan (HKH) region under medium-range (RCP4.5) and high-end (RCP8.5) emissions scenario forcing conditions. The ensemble of multi-RCM outputs analysed is developed based on the CORDEX framework, which includes three modelling centres in different countries. These RCMs are run over a common domain covering South Asia with 50 km spatial resolution. This study provides the baseline for assessing the future changes in the seasonal mean surface air temperature and precipitation, which will be useful in interpreting the projected changes in climatic extremes over the HKH region.

The CORDEX South Asia multi-RCM simulated ensemble mean 2-m air temperature seasonal climate for the recent past period (1976–2005) showed large cold bias over HKH region during summer monsoon and winter seasons relative to the APHRODITE gridded analyses of station observations. Detailed analysis for the three hilly sub-regions within HKH indicated that the downscaled RCMs have relatively higher cold bias than the AOGCMs. The spread among these multi-RCM simulated winter season temperatures are also found to be higher than for the AOGCMs. The spatial distribution of the RCM ensemble mean indicated wet bias over the HKH region during both seasons expect for the higher elevated regions in south-east Himalaya and the Tibetan Plateau (HKH3) during summer season. However the detailed boxplot analysis in the hilly sub-regions within HKH showed that the RCMs and the AOGCMs overestimate the ensemble median total precipitation in all these sub-regions during both the seasons. The RCM ensemble median was found to be relatively closer to observations than for the AOGCMs over the central Himalaya (HKH2) and HKH3 for both seasons, and was also found to be associated with smaller inter-model variability over HKH2 during the summer monsoon season.

Table 4
CMIP5 global seasonal ensemble mean projected changes in near-surface air temperature (°C) relative to 1976–2005.

Period	Summer monsoon season (June–September)		Winter season (December–February)	
	RCP4.5	RCP8.5	RCP4.5	RCP8.5
2036–2065	1.4	1.9	1.5	2.0
2066–2095	1.9	3.3	2.0	3.5

The summer monsoon (winter) season warming over the hilly sub-regions in HKH for both future periods and scenarios are found to be relatively lower (higher) for the RCMs than for the AOGCMs in the analysis of the spatial pattern of these multi-model ensemble means and for the multi-model ensemble median values using boxplot analysis. The multi-RCM ensemble mean projected summer temperature changes for far-future period (2066–2095) under RCP8.5 scenario indicates that relatively higher warming of 4.9 °C will occur over the hilly regions of northwest Himalaya and Karakoram (HKH1) than of 4.2 °C over HKH3, with lower uncertainty for RCMs, particularly over HKH1. The boxplot analysis also bring out the relatively better confidence provided by the high resolution RCMs than the coarser AOGCMs in projecting relatively higher RCM ensemble mean winter warming of 5.4 °C (Table 2) for hilly region within HKH1 compared to the summer monsoon season by the end of 21st century under RCP8.5 scenario. However it is found that the highest winter warming for this high-end scenario in the far future period indicated by the RCM ensemble mean over the hilly region within HKH2 is associated with large uncertainty.

The ensemble mean of the high resolution RCMs and the coarser AOGCMs indicate similar variations in the projected summer monsoon season total precipitation changes across these HKH sub-regions for both periods and scenarios. The RCMs indicate that during summer (winter) relatively higher (lower) precipitation increase will occur over the hilly regions of central Himalaya and southeast Himalaya and Tibetan Plateau than in northwest Himalaya and Karakoram for both scenarios by the end of 21st century. The finding that the highest intensification of the summer monsoon precipitation of about 22% will occur over the hilly regions within HKH3 for RCP8.5 scenario is supported by good consensus among the RCMs and low uncertainty. These RCMs indicate poor consensus on the projected increase in summer monsoon precipitation in the hilly regions within HKH1 and HKH2, particularly with higher inter-RCM variability over HKH2. The precipitation change in the wetter cold season shows an increase of 13%–14% by the end of 21st century over the hilly regions within HKH1 with consensus among the individual RCMs for both scenarios. However this result is accompanied with moderate uncertainty as indicated by the inter-model spread in the projected changes. Further, the consensus

among the downscaled RCMs for projected reduction in winter precipitation over HKH2 and HKH3 are also low for both scenarios in the two future periods.

This study indicates that the uncertainty in the projected changes for the sub-regions within HKH arising from individual models and scenarios are larger by the end of 21st century as shown by the divergence among the RCMs, particularly for the hilly regions of central Himalaya, which is influenced by both the South Asian summer monsoon and the passage of winter westerly disturbances. Hawkins and Sutton (2011) had reported that the contribution from model uncertainty dominates the total uncertainty in the CMIP5 AOGCM projections over India by the end of this century. The South Asian summer monsoon remains a complex phenomenon influenced by several regional factors such as aerosols, land cover and land-use, and Indian Ocean temperature (Krishnan et al., 2016). Although the CMIP5 AOGCMs have implemented these regional forcing with varying degree of complexity, the RCMs used to downscale the CMIP5 projections for CORDEX South Asia does not include these regional scale forcings. Therefore, these downscaled projected changes need to be taken with caution and demands detailed understanding of such processes and feedbacks.

The analysis presented in this study quantified separately the model performance in reproducing the observed seasonal climatology over the hilly sub-regions within HKH and the deviation of the individual projection of future change with respect to the multi-model ensemble average. The reliability of these climate change projections for HKH can be further enhanced by assigning larger weights to the models with smaller bias and with future projected change closer to the ensemble mean. We will explore such methods for quantifying the uncertainty and reliability associated with climate model projections in future studies, as the consideration of model uncertainty using multi-model outputs will provide confidence to decision-makers in formulating policies for climate change impact assessment in the Hindu Kush Himalayan region.

Acknowledgments

The IITM-RegCM4 simulations were performed using the IITM Aaditya high power computing resources. The Director, IITM is gratefully acknowledged for extending full support to carry out this research work. IITM receives full support from the Ministry of Earth Sciences, Government of India. The World Climate Research Programme's Working Group on Regional Climate, and the Working Group on Coupled Modelling, former coordinating body of CORDEX and responsible panel for CMIP5 are sincerely acknowledged. The climate modelling groups (listed in Table 1) are sincerely thanked for producing and making available their model output. The Earth System Grid Federation infrastructure (ESGF; http://esgf.llnl.gov/index.html) is also acknowledged. The Climate Data Operators software (CDO; https://code.zmaw.de/projects/cdo/) and the Grid Analysis and Display System (GrADS; http://iges.org/grads/) were extensively used throughout this analysis. The authors would like to thank two anonymous reviewers for their helpful comments and suggestions.

References

Barnett, T.P., Adam, J.C., Lettenmaier, D.P., 2005. Potential impacts of a warming climate on water availability in snow-dominated regions. Nature 438, 303−309.

Bookhagen, B., Burbank, D.W., 2010. Toward a complete Himalayan hydrological budget: spatiotemporal distribution of snowmelt and rainfall and their impact on river discharge. J. Geophys. Res. Earth 115, F03019. http://dx.doi.org/10.1029/2009JF001426.

Dee, D.P., Uppala, S.M., Simmons, A.J., et al., 2011. The ERA-Interim reanalysis: configuration and performance of the data assimilation system. Q. J. R. Meteorol. Soc. 137, 553−597. http://dx.doi.org/10.1002/qj.828, 2011.4757, 4759, 4775.

Dimri, A.P., Yasunari, T., Wiltshire, A., et al., 2013. Application of regional climate models to the Indian winter monsoon over the western Himalayas. Sci. Total Environ. 468−469. http://dx.doi.org/10.1016/j.scitotenv.2013.01.040. S36−S47.

Flato, G.J., et al., 2013. Evaluation of climate models. In: Stocker, T.F., Qin, D., Plattner, G.-K., et al. (Eds.), Climate Change 2013: The Physical Science Basis. Contribution of Working Group I to the Fifth Assessment Report of the Intergovernmental Panel on Climate Change. Cambridge University Press, Cambridge and New York, pp. 741−866.

Giorgi, F., Coppola, E., Solmon, F., et al., 2012. RegCM4: model description and preliminary tests over multiple CORDEX domains. Clim. Res. 52, 7−29. http://dx.doi.org/10.3354/cr01018.

Hawkins, E., Sutton, R., 2011. The potential to narrow uncertainty in projections of regional precipitation change. Clim. Dyn. 37, 407−418. http://dx.doi.org/10.1007/s00382-010-0810-6.

Jacob, D., Elizalde, A., Haensler, A., et al., 2012. Assessing the transferability of the regional climate model REMO to different coordinated regional climate downscaling experiment (CORDEX) regions. Atmosphere 3, 181−199.

Kapnick, S.B., Delworth, T.L., Ashfaq, M., et al., 2014. Snowfall less sensitive to warming in Karakoram than in Himalayas due to a unique seasonal cycle. Nat. Geosci. 7 (11), 834−840.

Krishnan, R., Sabin, T.P., Vellore, R., et al., 2016. Deciphering the desiccation trend of the South Asian monsoon hydroclimate in a warming world. Clim. Dyn. 47, 1007−1027. http://dx.doi.org/10.1007/s00382-015-2886-5.

Palazzi, E., von Hardenberg, J., Provenzale, A., 2013. Precipitation in the Hindu-Kush Karakoram Himalaya: observations and future scenarios. J. Geophys. Res. Atmos. 118, 85−100. http://dx.doi.org/10.1029/2012JD018697.

Panday, P.K., Thibeaultb, J., Freyc, K.E., 2015. Changing temperature and precipitation extremes in the Hindu Kush-Himalayan region: an analysis of CMIP3 and CMIP5 simulations and projections. Int. J. Climatol. 35, 3058−3077. http://dx.doi.org/10.1002/joc.4192.

Samuelsson, P., Jones, C.G., Willen, U., et al., 2011. The Rossby Centre Regional Climate model RCA3: model description and performance. Tellus 63A, 4−23. http://dx.doi.org/10.1111/j.1600-0870.2010.00478.x.

Sanjay, J., Ramarao, M.V.S., Mujumdar, M., et al., 2017. Regional climate change scenarios. In: Rajeevan, M.N., Nayak, Shailesh (Eds.), Chapter of Book: Observed Climate Variability and Change over the Indian Region. Springer Geology, pp. 285−304. http://dx.doi.org/10.1007/978-981-10-2531-0.

Shrestha, A.B., Devkota, L.P., 2010. Climate Change in the Eastern Himalayas: Observed Trends and Model Directions. Climate Change Impact and Vulnerability in the Eastern Himalayas. ICIMOD, Kathmandu. Technical Report 1.

Taylor, K.E., Stouffer, R.J., Meehl, G.A., 2012. An overview of CMIP5 and the experiment design. Bull. Amer. Meteor. Soc. 93, 485−498.

Teichmann, C., Eggert, B., Elizalde, A., et al., 2013. How does a regional climate model modify the projected climate change signal of the driving

GCM: a study over different CORDEX regions using REMO. Atmosphere 4 (2), 214−236. http://dx.doi.org/10.3390/atmos4020214.

Wiltshire, A.J., 2014. Climate change implications for the glaciers of the Hindu Kush, Karakoram and Himalayan region. Cryosphere 8, 941−958. http://dx.doi.org/10.5194/tc-8-941-2014.

Yasutomi, N., Hamada, A., Yatagai, A., 2011. Development of a long-term daily gridded temperature dataset and its application to rain/snow discrimination of daily precipitation. Glob. Environ. Res. 15, 165−172.

Yatagai, A., Kamiguchi, K., Arakawa, O., et al., 2012. APHRODITE: constructing a long-term daily gridded precipitation dataset for Asia based on a dense network of rain gauges. Bull. Am. Met. Soc. 93, 1401−1415. http://dx.doi.org/10.1175/BAMS-D-11-00122.1.